Infrared Radiation Confers Resistance to UV-Induced Apoptosis *Via* Reduction of DNA Damage and Upregulation of Antiapoptotic Proteins

Christian Jantschitsch[1], Sebastian Majewski[1], Akira Maeda[1], Thomas Schwarz[1] and Agatha Schwarz[1]

Infrared radiation (IR) is increasingly used for wellness purposes. In this setting, it is frequently combined with UV radiation, primarily for tanning purposes. The impact of IR on UV-induced carcinogenesis is still unclear. Hence, we investigated the interplay between IR and UV with regard to UV-induced apoptosis. Pretreatment of murine keratinocytes with IR before UV reduced the apoptotic rate. Likewise, the number of sunburn cells was reduced in mice preexposed to IR before UV. The amounts of UV-induced DNA damage were reduced by IR both *in vitro* and *in vivo*. This was not observed in DNA repair-deficient mice. UV-induced downregulation of the antiapoptotic proteins $FLIP_L$ and $BCL-X_L$ was prevented by IR, whereas the proapoptotic protein BAX was downregulated. These data indicate that IR reduces UV-induced apoptosis that may be mediated by several pathways, including reduction of DNA damage and induction of antiapoptotic proteins. The antiapoptotic effects of IR may support the survival of UV-damaged cells and thus carcinogenesis. As, however, IR reduces UV-induced DNA damage, the balance between these two effects may be important. Thus, *in vivo* carcinogenesis studies are required to define the role of IR and its interaction with UV in photocarcinogenesis.

INTRODUCTION

Upon exposure to solar radiation human skin is not only affected by UVB (290–320 nm) and UVA radiation (320–400 nm), but also by infrared radiation (IR). Owing to the multiple biologic effects of UV radiation, which include sunburn, photoallergic and phototoxic reactions, skin aging and induction of skin cancer, the vast majority of studies elucidating the impact of solar radiation on human health have almost exclusively concentrated on UV, whereas IR was almost ignored. In addition, for quite a long time it was assumed that IR does not exert any biological effects and thus may be irrelevant and innocuous to human skin. Unlike solar UV and visible light, IR is hardly absorbed by clouds, fog, and dust in the atmosphere. IR accounts for approximately 54% of the total solar energy reaching the earth's surface, whereas UV only for 7% (Kochevar *et al.*, 1999). Most of the IR lies within the IR-A range (760–1,400 nm) that accounts for approximately 30% of total solar energy. In contrast to IR-B (1,400–3,000 nm) and IR-C (3,000 nm–1 mm), IR-A deeply penetrates into human skin (Schroeder *et al.*, 2007). Thus, it is not surprising that biologic effects induced by IR-A in human skin have been described recently (reviewed in Schieke *et al.*, 2003).

One consequence of the recognition of biologic effects of IR-A is the administration of artificial IR-A for cosmetic and wellness purposes. This is based on the concept that IR-A and heat relax the skin and might contribute to a rejuvenation process. Although these anticipations have never been proven seriously, the frequency of IR-A exposures in the wellness business is rapidly rising. In this setting, IR-A treatments are often combined with artificial UV exposures, mostly for tanning purposes. It is generally accepted that excessive chronic UV exposure dramatically enhances the risk for skin cancer (Nishigori, 2006). Which impact additional IR-A exposure might have is quite unclear but an obvious concern of the public health-care authorities. This is quite comprehensible in view of the postulation that the incidence of skin cancer may be augmented by rising temperatures as a consequence of the climate change (Owens and Knox, 1978; van der Leun and de Gruijl, 2002).

UV-mediated apoptosis is regarded as a protective mechanism preventing malignant transformation by eliminating cells that carry high loads of UV-induced DNA damage. Owing to its protective function, alterations in UVB-induced apoptosis may have profound impact in the induction of skin cancer (Nickoloff *et al.*, 2002). To get a first idea how artificial IR-A might influence photocarcinogenesis, we studied as a first step the effect of IR-A on UV-induced

[1]Department of Dermatology, University Kiel, Kiel, Germany

Correspondence: Dr Thomas Schwarz, Department of Dermatology, University Kiel, Schittenhelmstrasse 7, Kiel 24105, Germany. E-mail: tschwarz@dermatology.uni-kiel.de

Figure 1. **Pretreatment with IR-A reduces UVB-induced apoptosis in murine keratinocytes.** Cells were pretreated with IR-A ($250 \, \text{J cm}^{-2}$) and 3 hours later irradiated with UVB ($55 \, \text{mJ cm}^{-2}$). At 16 hours after UVB irradiation, the apoptotic rate was determined using a cell death ELISA. Bars represent the mean ± SD absorbance (optical density, OD) of duplicates of one representative of three independent experiments. *$P<0.0005$ vs UVB only.
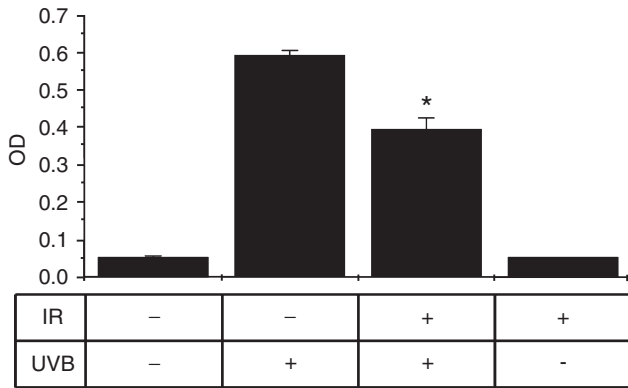

Figure 2. **Pretreatment with IR-A reduces FasL-induced apoptosis in murine keratinocytes.** Cells were pretreated with IR-A ($250 \, \text{J cm}^{-2}$) and 3 hours later incubated with $75 \, \text{ng ml}^{-1}$ FasL. After 16 hours of incubation, the apoptotic rate was determined using a cell death ELISA. Bars represent the mean ± SD absorbance (optical density, OD) of duplicates of one representative of three independent experiments. *$P<0.0005$ vs FasL without IR-A pretreatment.

apoptotic cell death of keratinocytes. We demonstrate that exposure to IR-A before UV reduces apoptotic cell death both *in vitro* and *in vivo* that might be mediated by several pathways including reduction of DNA damage and modulation of antiapoptotic proteins.

RESULTS

IR-A reduces UVB-induced apoptosis *in vitro*
To determine the effect of IR-A on UVB-induced apoptosis, keratinocytes obtained from ear sheets of C57BL/6N mice were exposed to $250 \, \text{J cm}^{-2}$ IR-A. At 3 hours later, cells were irradiated with $55 \, \text{mJ cm}^{-2}$ UVB. At 16 hours later, apoptosis was determined using a cell death detection ELISA. UVB alone resulted in an increased apoptotic rate (Figure 1). In contrast, in cells that were preexposed to IR-A apoptosis was significantly reduced, when compared to UVB only treated keratinocytes. IR-A alone did not induce apoptosis.

IR-A protects from apoptosis induced by Fas–FasL interaction
UV-induced apoptosis is a complex process involving release of cytochrome *C* from mitochondria, activation of p53 by nuclear DNA damage, and activation of death receptors either by causing receptor clustering or by inducing death ligands (Kulms *et al.*, 2002). Hence, we tested the effect of IR-A pretreatment on FasL-induced apoptosis in which the pathways involved are less heterogeneous. Freshly prepared murine keratinocytes were pretreated with $250 \, \text{J cm}^{-2}$ 3 hours before addition of FasL ($75 \, \text{ng ml}^{-1}$) to the culture medium. At 16 hours later, the apoptotic rate was determined using a cell death detection ELISA. Comparable to UV-induced cell death, FasL-mediated apoptosis was significantly decreased by IR-A pretreatment (Figure 2).

Pretreatment with IR-A reduces UVB-induced apoptosis *in vivo*
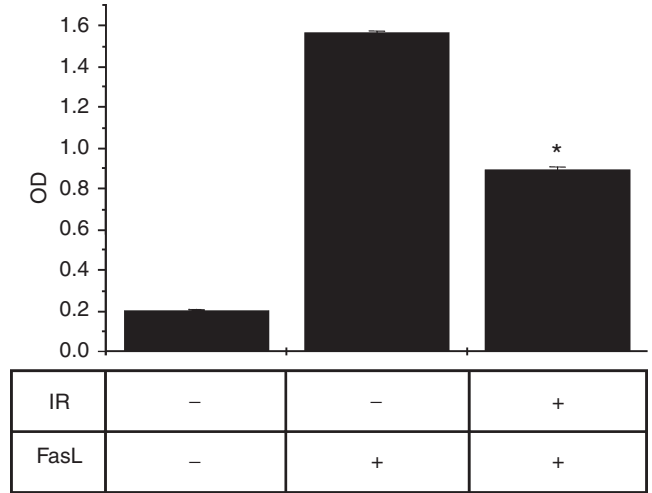To investigate the impact of IR-A on UVB-induced apoptosis *in vivo*, the effect of IR-A on the formation of apoptotic keratinocytes (sunburn cells) was analyzed. Mice were exposed to $135 \, \text{J cm}^{-2}$ IR-A on the shaved backs. At 3 hours later the animals were irradiated with $150 \, \text{mJ cm}^{-2}$ UVB. At 16 hours later, punch biopsies were taken from the UV-exposed skin areas. Biopsies were fixed and tissue sections stained with hematoxylin and eosin. The number of sunburn cells in the epidermis, characterized as epidermal cells with a pycnotic nucleus and a shrunken eosinophilic cytoplasm, was evaluated. In mice that had been pretreated with IR-A before UV exposure, the number of sunburn cells was significantly lower than that found in animals that were only UVB treated (Figure 3). IR-A on its own did not induce sunburn cells.

IR-A pretreatment reduces UVB-induced DNA damage *in vitro* and *in vivo*
One of the major molecular triggers for UV-induced apoptosis is UV-induced DNA damage as reduction of DNA damage is associated with a decrease of the apoptotic rate (Kulms *et al.*, 1999). UVB induces primarily two types of DNA lesions, cyclobutane pyrimidine dimers (CPDs) and 6–4 photoproducts. Hence, the amounts of CPDs were determined by Southwestern dot-blot analysis. Murine keratinocytes were pretreated with $250 \, \text{J cm}^{-2}$ IR-A 3 hours before UVB irradiation. At 4 hours later, DNA was extracted, blotted, and subjected to staining with an antibody directed against CPDs. No CPDs were detected in unirradiated cells. CPDs were clearly detectable in cells exposed to UVB. Preexposure to IR-A remarkably reduced the amounts of CPDs. IR-A on its own did not induce CPDs. Densitometry analysis of four independent experiments revealed that IR-A pretreatment decreased the amounts of CPDs by $52.2 \pm 13.0\%$ (mean ± SD).

To evaluate the *in vivo* relevance of these findings, mice were exposed on their shaved backs to $135 \, \text{J cm}^{-2}$ IR-A. At
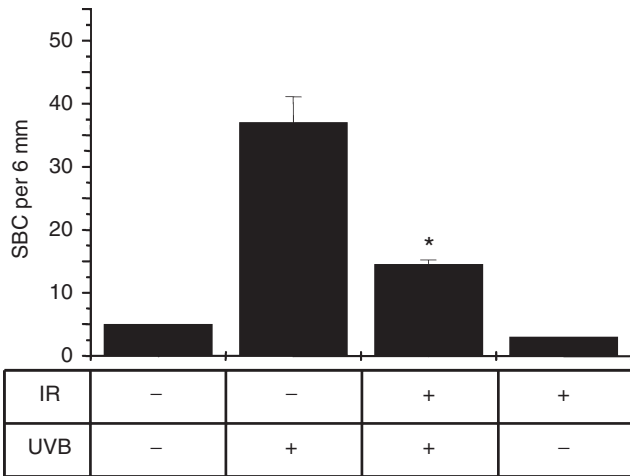
Figure 3. Pretreatment with IR-A reduces sunburn cell formation in murine epidermis. C57BL/6N mice were pretreated with $135 \, J \, cm^{-2}$ IR-A on their shaved backs 3 hours before irradiation with $150 \, mJ \, cm^{-2}$ UVB. At 16 hours later, punch biopsies were taken, sections cut, and stained with H&E. Sunburn cells (SBC) were defined as epidermal cells with a pycnotic nucleus and a shrunken eosinophilic cytoplasm. The number of SBC per 6 mm in length of epidermis was counted. The bars show the mean ± SD of at least three different sections of one representative of three independent experiments. *$P < 0.05$ vs only UVB-treated mice.

3 hours later, the same areas were irradiated with $75 \, mJ \, cm^{-2}$ UVB. At 16 hours later, punch biopsies were taken from the exposed skin areas. Skin sections were subjected to immunohistochemistry using the antibody directed against CPDs. In samples of mice exposed to UVB only, the vast majority of epidermal cells revealed a nuclear staining, indicative of DNA damage. The staining was reduced by 46% in samples obtained from mice that were exposed to IR-A before UVB (Figure 4a).

To differentiate whether IR-A prevents the formation of CPDs, the experiment was repeated but this time biopsies were taken immediately after UV exposure. In this case, no significant differences between UVB only and UVB plus IR-A-exposed skin samples were detectable (Figure 4b). Thus immediately after UV exposure the amounts of CPDs appear to be the same irrespective of IR-A preexposure, excluding that IR-A prevents the formation of CPDs.

The fact that the amounts of UVB-induced DNA damage were the same in the IR-A-treated and untreated skin samples immediately after UVB exposure but reduced by IR-A preexposure at later time points implies that IR-A might support the removal of UVB-induced DNA lesions. This can be achieved by inducing DNA repair. UVB-mediated DNA damage is repaired by the nucleotide excision repair (NER; de Laat *et al.*, 1999). To elucidate whether NER is involved in the reduction of CPDs caused by IR-A, the *in vivo* experiments were performed with *Xpa* knockout mice that are deficient in NER (de Vries *et al.*, 1995). *Xpa* knockout mice were exposed to $135 \, J \, cm^{-2}$ IR-A followed by $55 \, mJ \, cm^{-2}$ UVB 3 hours later. At 16 hours thereafter, punch biopsies were taken from UV-exposed skin and stained for CPDs. In
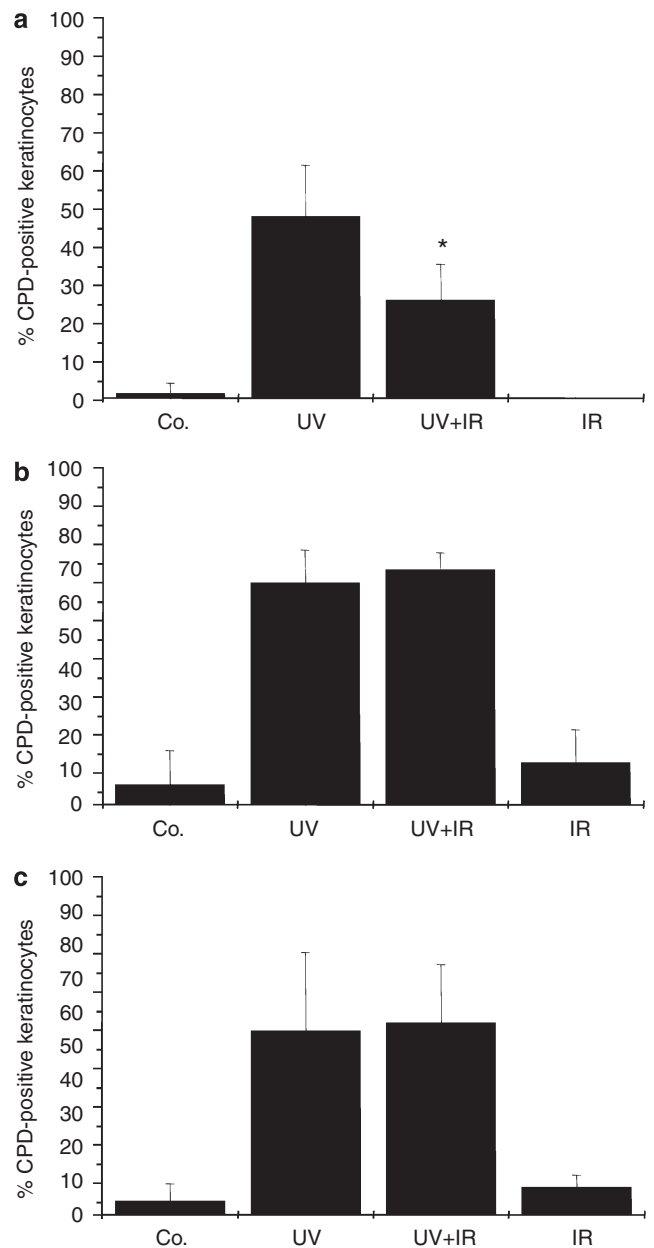

Figure 4. IR-A reduces pyrimidine dimers *in vivo*. (a) C57BL/6N mice were pretreated with $135 \, J \, cm^{-2}$ IR-A 3 hours before irradiation with $75 \, mJ \, cm^{-2}$ UVB. At 16 hours later, punch biopsies were taken and *in situ* staining using a monoclonal antibody against pyrimidine dimers was performed. (b) Mice were treated identically as in (a) but punch biopsies were taken immediately after UVB exposure. (c) *Xpa* knockout mice were pretreated with $135 \, J \, cm^{-2}$ IR-A 3 hours before irradiation with $55 \, mJ \, cm^{-2}$ UVB. At 16 hours, later punch biopsies were taken and *in situ* staining using a monoclonal antibody against CPDs was performed. From each sample of two independently performed experiments, three randomly chosen lengths of $630 \, \mu m$ epidermis were evaluated for the percentage of CPD-positive cells (mean ± SD). *$P < 0.01$ vs UV.

contrast to the findings with wild-type mice, IR-A pretreatment did not reduce the CPD staining (Figure 4c). This implies that NER appears to be involved in the reduction of UV-induced DNA damage by IR-A pretreatment.

IR-A reduces UV-induced DNA damage in the shuttle vector assay

The observations that IR-A reduces UV-induced DNA damage both *in vitro* and *in vivo* and that this effect may be linked to NER were quite surprising. To consolidate the involvement of DNA repair in this scenario, the shuttle vector assay was used. A chloramphenicol acetyltransferase (CAT) reporter construct was exposed to UV. Subsequently, the vector was transfected into PAM 212 cells via electroporation. One group of PAM 212 cells was exposed to $250 \, \mathrm{J \, cm^{-2}}$ IR-A 3 hours before transfection. At 16 hours after transfection, the CAT enzyme activity was determined using a CAT-ELISA. Cells that received the UV-damaged plasmid exhibited a significantly reduced CAT activity compared to cells having received the unirradiated plasmid (Figure 5). In contrast, CAT activity was significantly enhanced in cells that had been exposed to IR-A before receiving the UV-exposed construct. As the reduction of CAT activity correlates with the severity of DNA damage and all constructs were exposed to the same UVB dose, the results of the shuttle vector assay support the hypothesis that IR-A might induce DNA repair.

IR-A pretreatment affects the expression of apoptosis-related proteins

The data obtained so far suggest that one mechanism by which IR-A reduces UV-induced apoptosis is reduction of DNA damage. However, the fact that IR-A also reduces FasL-induced apoptosis (Figure 2) indicates that other mechanisms have to be involved as well, because DNA damage does not play a role in FasL-mediated apoptosis. Thus, the effect of IR-A on the expression of the antiapoptotic proteins $FLIP_L$ and $BCL-X_L$ was studied. Murine keratinocytes were exposed to UVB with and without IR-A pretreatment, harvested 16 hours after UV exposure, permeabilized, and subjected to intra-cellular staining with antibodies directed against $FLIP_L$ and $BCL-X_L$. Staining intensity was evaluated by FACS analysis.

UVB downregulated both $FLIP_L$ and $BCL-X_L$ (Figure 6). When cells were pretreated with $250 \, \mathrm{J \, m^{-2}}$ IR-A 3 hours before UVB, the UVB-induced downregulation was prevented. Analysis of the expression of the proapoptotic protein BAX revealed a downregulation by IR-A (Figure 6).

IR-A affects both intrinsic and extrinsic apoptosis

To confirm the assumption that IR-A pretreatment might influence the intrinsic/mitochondrial as well as the extrinsic/death-receptor-mediated apoptotic pathway in a prosurvival pattern, activation of caspase-8 as a parameter for the extrinsic and of caspase-9 as a parameter for the intrinsic pathway was determined. IR-A pretreatment inhibited UVB-induced increase of both caspases-8 and -9 activity (Figure 7). This suggests that both pathways are affected by IR-A.

IR-A does not induce heat-shock protein 70

It is known that the induction of heat-shock proteins, in particular Hsp70, inhibits UVB-induced apoptosis in keratinocytes (Trautinger *et al.*, 1995). Hence, the question is obvious whether IR-A exerts its antiapoptotic effect by simply inducing Hsp70. To address this issue, murine keratinocytes were exposed to either IR-A ($250 \, \mathrm{J \, cm^{-2}}$) or heat-shock (3 hours at $42 \, ^\circ \mathrm{C}$ followed by a recovery phase of 3 hours at $37 \, ^\circ \mathrm{C}$). Cells were harvested and Hsp70 expression measured with an Hsp70 ELISA. Heat shock strongly induced Hsp70, whereas IR-A treatment did not significantly increase Hsp70 (Figure 8).

DISCUSSION

In contrast to the detailed knowledge about the biological effects of UV and their impact on human health, not much is known about the response to IR. This may appear surprising as human skin is increasingly exposed to IR from both natural and artificial sources. For a long time, IR was regarded as biologically inert and thus not included in detailed studies. However, there is accumulating evidence that IR, in particular IR-A, is able to exert biologic effects on human skin. It may cause and enhance premature aging and carcinogenesis (Kligman, 1982; Dover *et al.*, 1989; Schieke *et al.*, 2002; Kim *et al.*, 2005, 2006; Cho *et al.*, 2008). Moreover, it has been published that IR-A indirectly exerts antioxidative properties because of its ability to induce ferritin, which reduces free iron and thus free radicals (Applegate *et al.*, 2000). IR is used for cosmetic and wellness purposes even for local fat and body weight reduction (Möckel *et al.*, 2006) and for the therapy of various diseases including wound healing processes (Horwitz *et al.*, 1999; Danno *et al.*, 2001; Schramm *et al.*, 2003), autoimmune and inflammatory disorders (Meffert *et al.*, 1990; Yokoyama and Oku, 1999), and malignant diseases (Dees *et al.*, 2002).

There is recent concern about the interaction between UV and IR with regard to carcinogenesis. This is based on the fact that prolonged natural solar exposure is associated with an increase of the cumulative load not only of UV but also of IR. The current discussion that the rise of the environmental
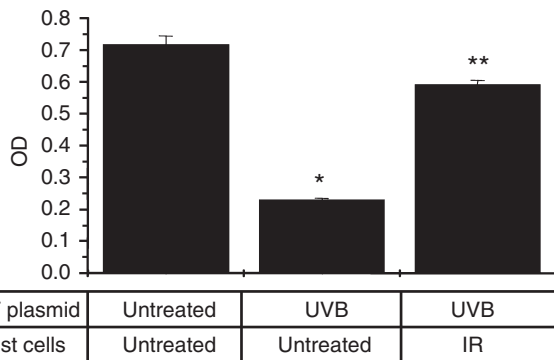

Figure 5. **IR-A restores UV-suppressed CAT activity in the shuttle vector assay.** PAM 212 cells were either left untreated or were exposed to $250 \, \mathrm{J \, cm^{-2}}$ IR-A. At 3 hours later, cells were transfected by electroporation with a CAT-plasmid vector that had been exposed to $30 \, \mathrm{mJ \, cm^{-2}}$ UVB. Control cells were left untreated and transfected with a CAT plasmid that was not exposed to UV. At 16 hours after transfection, CAT enzyme activity was measured using a CAT-ELISA. Bars show the mean ± SD absorbance (optical density, OD) of duplicates of one representative of three independent experiments. *$P < 0.005$ vs cells transfected with untreated CAT plasmid. **$P < 0.005$ vs untreated cells transfected with UVB-irradiated CAT plasmid.
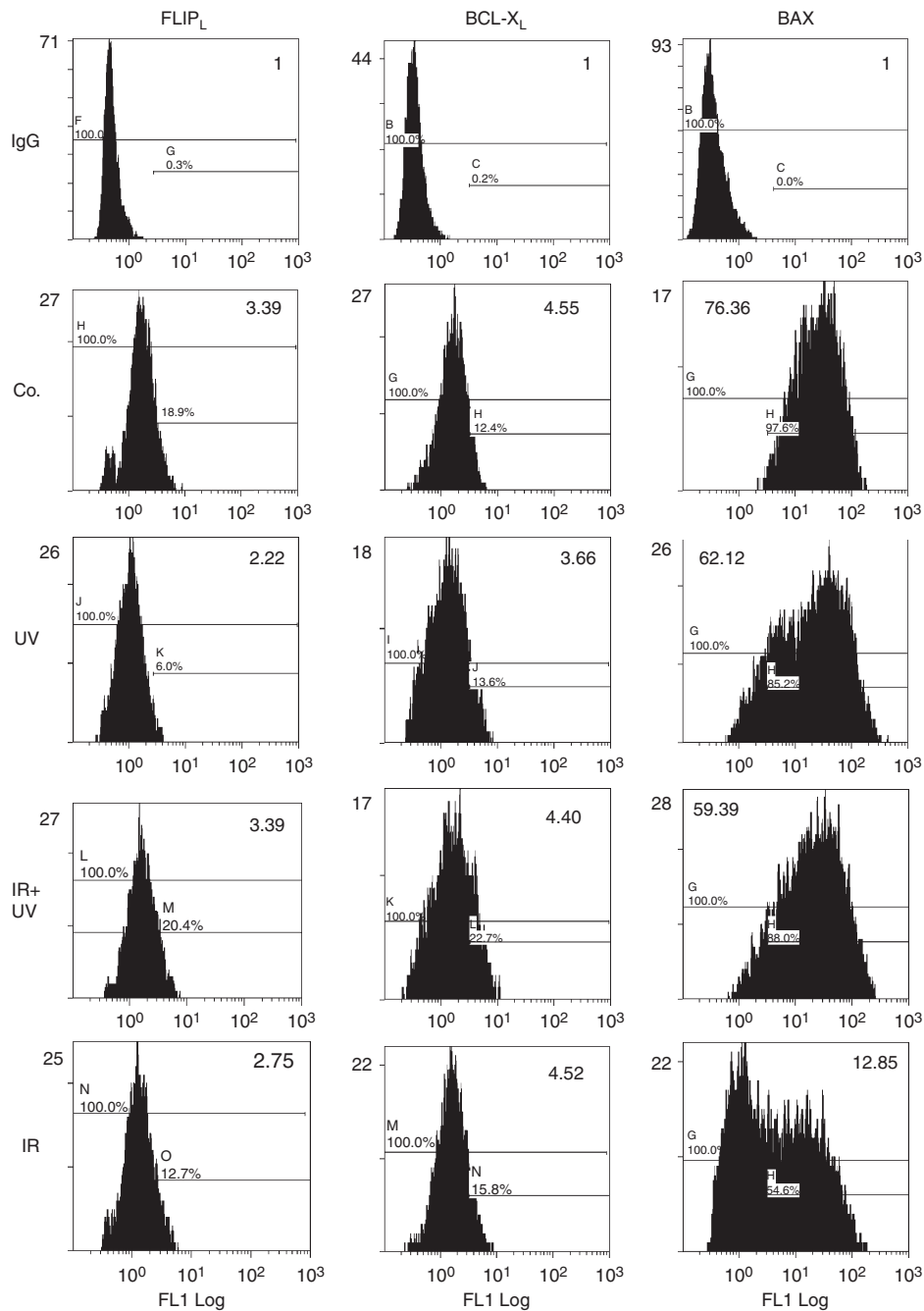
Figure 6. **Pretreatment of murine keratinocytes with IR-A restores UVB-induced downregulation of the antiapoptotic proteins FLIP$_L$ and BCL-X$_L$ and downregulates the proapoptotic protein BAX.** Murine keratinocytes were either left untreated (Co.), irradiated with UVB (55 mJ cm^{-2}) only (UV), pretreated with 250 J cm^{-2} IR-A before UVB exposure (IR + UV), or with IR-A alone (IR). At 16 hours after irradiation, cells were harvested, permeabilized, stained with antibodies against FLIP$_L$, BCL-X$_L$, or BAX and subjected to FACS analysis. Histograms show fluorescence intensity (*x* axis) versus cell number (*y* axis). The values in the respective histograms indicate the *x*-median values normalized to the IgG control that was arbitrarily set as 1. Shown is one representative of three independently performed experiments.

temperature because of the climate change may increase the risk for photocarcinogenesis (van der Leun and de Gruijl, 2002), initiated the debate of the necessity to protect not only from UV but also from IR (Schroeder *et al*., 2007). The fact that in the wellness business, IR is quite frequently combined with artificial UV exposures for tanning purposes adds to this discussion.

Experimental data about the interaction of IR and UV in carcinogenesis are minimal. To elucidate this issue, we studied the effect of IR on UV-induced apoptosis. The rationale for this study was several fold. First, UV-induced apoptosis is regarded as a protective mechanism that may prevent malignant transformation (Nickoloff *et al*., 2002). Hence, alterations in the outcome of UV-induced apoptosis
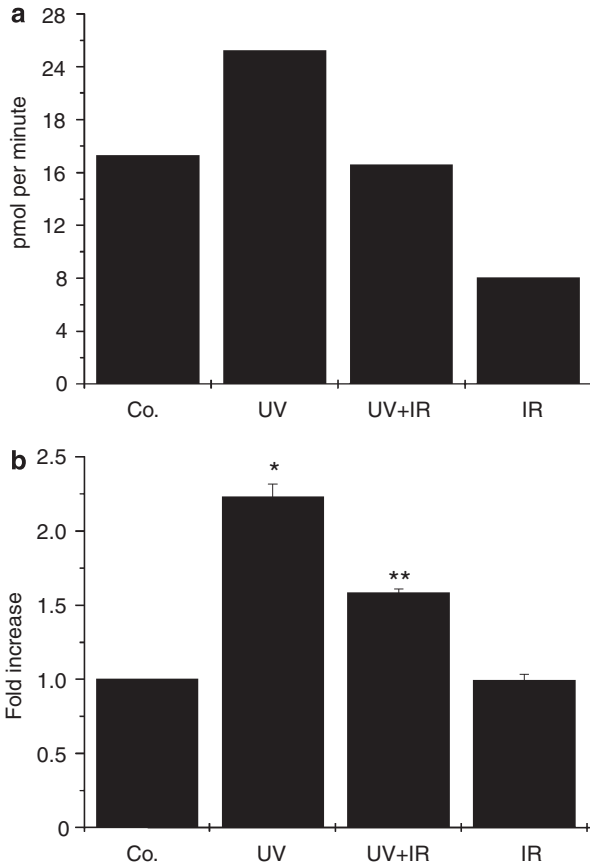
Figure 7. **IR-A pretreatment inhibits UV-induced increase of caspase-8 and caspase-9 activity.** PAM 212 cells were either left untreated (Co.), irradiated with UVB ($30\,mJ\,cm^{-2}$) only (UV), pretreated with $250\,J\,cm^{-2}$ IR-A before UVB exposure (IR + UV), or with IR-A alone (IR). At 16 hours after irradiation, cells were harvested and subjected either to a caspase-8 or to a caspase-9 assay. (**a**) Caspase-8 activity was determined from the slope calculated from the absorbance at 405 nm measured every minute over 10 minutes. Bars depict activity in pmol per minute of one representative of two independent experiments. (**b**) Bars show fold increase (mean ± SD of duplicates) compared to the caspase-9 activity of untreated control cells that was arbitrarily set as 1. Shown is one representative of two independently performed experiments. *$P < 0.005$ vs Co., **$P < 0.01$ vs UV.
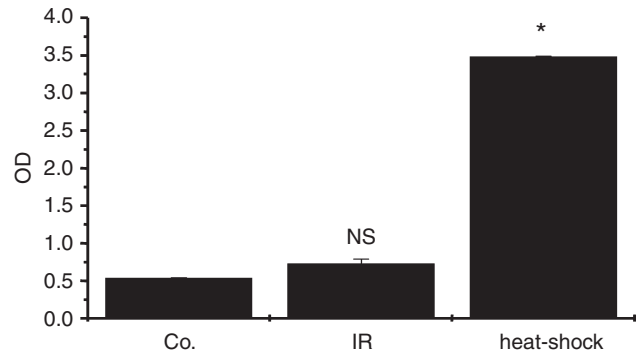

Figure 8. **IR-A does not induce Hsp70.** Murine keratinocytes were either left untreated (Co.), irradiated with $250\,J\,cm^{-2}$ IR-A, or exposed to heat-shock (42 °C for 3 hours). At 3 hours after IR-A treatment (IR) or heat-shock exposure, cells were harvested and Hsp70 protein expression was determined using an ELISA. Bars show the mean ± SD absorbance (optical density, OD) of duplicates of one representative of three independent experiments. *$P < 0.00005$ vs Co.

might have an impact on photocarcinogenesis. Second, heat exposure inhibits UV-induced apoptosis (Trautinger *et al.*, 1995). This observation is quite often quoted in the context that increases in temperature might enhance carcinogenesis (Owens and Knox, 1978; Dover *et al.*, 1989). However, the data obtained with heat exposure cannot be extrapolated for IR. IR-A reaches the subcutaneous tissue without substantially increasing the surface temperature of the skin, whereas IR-C is completely absorbed in the epidermis, thus causing rapid heating of the epidermis (Schieke *et al.*, 2003). In the present study, we utilized a water-filtered IR-A source. The water filter minimizes the heating effects of IR-A. Accordingly, we did not detect induction of heat-shock proteins such as Hsp70 upon exposure of cells to $250\,J\,cm^{-2}$ IR-A (Figure 8). As humans are exposed to an average IR dose of $75\,J\,cm^{-2}$ per hour (summertime, Munich, Germany; Schieke *et al.*, 2003), the doses of our *in vitro* experiments ($250\,J\,cm^{-2}$) resemble

approximately 3 hours outdoor stay. Although we initially planned to administer higher doses for the *in vivo* studies, we used only $135\,J\,cm^{-2}$ as it turned out that the long-exposure times required for the higher doses were technically not feasible without anesthesizing the mice.

The present data indicate that preexposure of murine keratinocytes to IR-A reduces UV-induced apoptosis. Upon *in vivo* exposure of mice to IR-A and UV, the number of apoptotic keratinocytes, visualized as sunburn cells, was significantly reduced. Danno *et al.* (1992) for the first time demonstrated *in vivo* that sunburn cell formation in mouse ear skin was significantly decreased by preexposure to IR. However, the type of IR applied in this study significantly elevated the surface temperature of ear lobes to 42 °C. Hence, this effect could have been mediated via induction of heat shock. Our *in vivo* data utilizing IR-A are of high relevance because of the recent debate whether *in vitro* data assessing the impact of IR-A are methodologically flawed and influenced by artifacts (Piazena and Kelleher, 2008; Schroeder and Krutmann, 2008).

The most surprising and unexpected finding of our study was the reduction of UV-induced DNA damage by pre-exposure to IR-A. This observation was made *in vitro* using Southwestern dot-blot analysis as well as by *in vivo* immunohistochemistry. Quantitative densitometric analysis indicated that IR-A might reduce the amounts of CPDs by around 50%. The same appears to apply for the *in vivo* situation. Careful analysis of the repair kinetic was not possible as we did not include several time points. However, the quantitative analysis of the *in situ* CPD staining (Figure 4) indicates that around 30% are removed within the first 16 hours and around 60% upon IR-A preexposure. The kinetic data are in accordance with the literature (Ruven *et al.*, 1993; Vink *et al.*, 1994). However, the data from different studies are difficult to compare as the repair kinetic is critically dependent on the UV dose, the mouse strain, and whether obtained *in vivo* or *in vitro*.

IR-A does not prevent the generation of CPDs, as biopsies obtained immediately after UV exposure did not reveal major differences in the amounts of CPDs. This indicated that the amounts of DNA damage from the beginning on are the same but become significantly less with time upon IR-A exposure. One explanation includes the possibility that the DNA damage is faster and/or more effectively removed upon IR-A exposure. The fact that these differences are not observed in *Xpa* knockout mice implies that the NER might be involved in this process. As IR-A does not reduce the amounts of CPDs in the *Xpa* knockout mice, one can assume that the number of sunburn cells might not be reduced in *Xpa* knockout mice by IR-A. Although we have not performed this experiment, this conclusion is valid, as the amounts of DNA damage are the major molecular trigger for UV-induced apoptosis (Kulms *et al.*, 1999). However, since IR-A also alters the expression of antiapoptotic proteins it cannot be excluded that this phenomenon might have an impact on the number of sunburn cells in repair-deficient mice as well. The involvement of DNA repair is also supported by the shuttle vector assay. The CAT activity was significantly enhanced when the UV-exposed plasmids were transfected into host cells that were preexposed to IR-A. Although both experiments do not definitely prove that IR-A exerts an effect on NER, they provide strong evidence for involvement of DNA repair in this process. It is not yet clear, whether IR-A affects the NER directly or indirectly for example via the release of mediators. In this context, it is important to mention that mediators released by keratinocytes including IL-12, IL-18, and α-melanocyte-stimulating hormone exhibit the capacity to reduce UV-induced DNA damage (Schwarz *et al.*, 2002, 2006; Böhm *et al.*, 2005).

Frank *et al.* (2006) reported that preirradiation with IR protects human fibroblasts from UV cytotoxicity *in vitro*. Similar to our study, this effect was not associated with heat-shock protein induction but dependent on p53 as p53-deficient SaOs cells were not rescued from UVB cytotoxicity by IR. The authors concluded that IR-induced p53 accumulation, stabilization, and phosphorylation prepare cells to better resist subsequent UV-induced stress. Preliminary experiments indicate that in our system p53 appears to be involved as well because HaCaT cells, a spontaneously transformed human keratinocyte cell line that carries two p53 mutations (Lehman *et al.*, 1993), were not protected from UVB-induced apoptosis by IR (data not shown). Nevertheless, further experiments investigating p53 stabilization and phosphorylation as well as examining the effect of p53 small-interfering RNA on the reduction of CPDs after IR-A would be necessary to support this hypothesis.

Despite the quite convincing data that IR-A inhibits UV-induced apoptosis by reducing DNA damage other pathways have to be involved as well. This assumption is based on the observation that IR-A also suppresses death ligand-induced apoptosis. As DNA damage does not play a role in this type of apoptotic cell death, we started to analyze the expression of anti- and proapoptotic proteins and whether their expression is influenced by IR-A. Intracellular FACS analysis revealed that IR-A reverts UV-induced downregulation of the antiapoptotic proteins $FLIP_L$ and $BCL-X_L$.

Furthermore, IR-A downregulated the proapoptotic BAX protein. This indicates that IR-A influences the intrinsic/mitochondrial apoptotic pathway as well as the extrinsic/death-receptor-mediated apoptotic pathway. This assumption was confirmed by showing that UVB-induced activation of caspase-8 (extrinsic pathway) as well as of caspase-9 (intrinsic pathway) was decreased by IR-A. This is in accordance with the previous observations that IR pretreatment of normal human fibroblasts inhibited UVB-induced activation of caspases-9 and -3 (Frank *et al.*, 1993, 2004). Whether this modulation by IR-A applies also for other apoptosis-related proteins remains to be determined. In addition, it is not yet clear, whether the modulation of these proteins by IR-A is of functional relevance. However, functional inhibition experiments using small-interfering RNA might not be indicative because of redundant pathways and consequently compensatory mechanisms.

Taken together, the present data indicate that IR-A reduces UV-induced apoptosis that may be mediated by several pathways including reduction of DNA damage and modulation of antiapoptotic proteins. The antiapoptotic effects of IR-A may support the survival of UV-damaged cells and thus carcinogenesis. As, however, IR-A reduces UV-induced DNA damage, the balance between these two effects may be important. Thus, *in vivo* carcinogenesis studies are required to define the definite role of IR-A and its interaction with UV in photocarcinogenesis.

MATERIALS AND METHODS
Cells and reagents
Freshly prepared murine keratinocytes obtained from ear sheets of 8- to 10-weeks-old female C57BL/6N mice were cultured in keratinocyte growth medium II with supplements (Promocell, Heidelberg, Germany). Cells of the transformed murine keratinocyte cell line PAM 212 were grown in RPMI 1640 culture medium containing 10% fetal calf serum and 1% glutamine (PAA, Linz, Austria). Human recombinant APO-1/Fas Ligand (Alexis, San Diego, CA) recognizing the human and mouse Fas receptor was used (75 ng ml^{-1} + enhancer 1 μg ml^{-1}).

Irradiation of cells
At 1 hour before irradiation with IR-A, medium was replaced either by keratinocyte growth medium II culture medium without supplements (keratinocytes) or by serum-free RPMI 1640 medium (PAM 212 cells). For irradiation with IR-A, medium was replaced by phosphate-buffered saline (PBS) at 37 °C. Subconfluent cells were exposed at a distance of 25 cm to a water-filtered IR-A irradiation source (Hydrosun-Strahler 505, Hydrosun Medizintechnik, Mühl-heim, Germany) equipped with a black cutoff filter emitting light in the range from 780 to 1,400 nm. After irradiation with IR-A, PBS was replaced either by keratinocyte growth medium II culture medium without supplements (keratinocytes) or by serum-free RPMI 1640 medium (PAM 212 cells). At 3 hours after IR-A treatment, cells were subjected to UVB from a bank of TL12 fluorescent lamps (Philips, Eindhoven, The Netherlands), which emit most of their energy within the UVB range (290–320 nm) with an emission peak at 313 nm. Cells were exposed to UVB in PBS at 37 °C. After UVB treatment, PBS was replaced by fresh keratinocyte growth medium II culture medium with supplements or RPMI 1640 culture medium containing 10% fetal calf serum and 1% glutamine.

Detection of cell death *in vitro*

At 16 hours after stimulation, cells were trypsinized from dishes and analyzed by a cell death detection ELISA (Cell death detection ELISA[plus], Roche Molecular Biochemicals, Mannheim, Germany). The enrichment of mono- and oligonucleosomes released into the cytoplasm of cell lysates is detected by biotinylated anti-histone- and peroxidase-coupled anti-DNA antibodies. Data are presented as the mean ± SD absorbance (optical density, OD) of one representative experiment out of three independently performed experiments. Statistical analysis was performed using the Student's *t*-test.

Flow cytometry

At 16 hours after irradiation, cells were harvested, fixed with 5.5% formaldehyde, permeabilized using 0.3% saponin, and incubated with the following first antibodies: affinity purified rabbit anti-human/mouse FLIP$_L$ (R&D Systems, Minneapolis, MN), polyclonal rabbit anti-mouse/rat BAX (BD Pharmingen, San Jose, CA), and polyclonal goat anti-mouse/human BCL-X$_L$ (Santa Cruz Biotechnologies, Santa Cruz, CA). Respective FITC-conjugated second step antibodies were used (FITC-conjugated rabbit anti-goat IgG (H + L) from Bethyl, Montgomery, TX and FITC-conjugated goat anti-rabbit IgG (H + L) from Biomeda, Burlingame, CA). Analysis was performed using a FC500 flow cytometer (Beckman Coulter) and CXP 2.2 software.

Measurement of caspase activity

At 16 hours after irradiation, activity of caspases was determined using caspases-8 and -9 assay kits (Calbiochem/Merck, Darmstadt, Germany). Cells were harvested and proteins purified. Protein concentration was measured using the Bradford method. 60 µg (caspase-8) or 150 µg (caspase-9) of total protein was subjected to the assay. Caspase-8 activity was determined according to the manufacturer's protocol. The slope was calculated from the absorbance at 405 nm measured every minute over 10 minutes. Results are presented as activity in pmol per minute. Caspase-9 activity is depicted as fold increase (mean ± SD of duplicates), calculated from the absorbance values compared to the activity of untreated control cells that were arbitrarily set as 1. One representative experiment of two independently performed experiments is shown.

Quantification of Hsp70

At 3 hours after irradiation with IR-A or exposure to 42 °C for 3 hours, cells were harvested, proteins were extracted according to a standard protocol, and protein concentration measured using the Bradford method. Total protein (10 µg) was subjected to a Hsp70 ELISA kit (Stressgen/Assay designs, Ann Arbor, MI). Data are demonstrated as the mean ± SD absorbance (OD) of one representative experiment out of three independently performed experiments. Statistical analysis was performed using the Student's *t*-test.

Southwestern dot-blot analysis

Genomic DNA was isolated from 10^6 cells according to the Puregene DNA extraction protocol (Gentra Systems, Minneapolis, MI). Non-denatured DNA (2 µg) was transferred to a positively charged nylon membrane by vacuum dot blotting and fixed by baking the membrane for 15 minutes at 80 °C. A monoclonal antibody directed against thymine dimers (Kamiya Biomedical Company, Seattle, WA) was used for Southwestern analysis.

Detection was carried out with a horseradish peroxidase-conjugated anti-mouse antibody. To ensure equal distribution of DNA, stripping with consecutive incubation with an antibody against adenosine (WAK-Chemie, Steinbach, Germany) was performed. Densitometry of the blots was performed using GeneTools software, version 3.06 (SynGene, Cambridge, UK).

Shuttle vector assay

The 4465 bp pCAT3-control vector (Promega Corp., Madison, WI) containing the gene for the enzyme CAT as an insert was irradiated with 30 mJ cm^{-2} UVB. UV-damaged plasmid (20 µg) were electroporated into 3×10^6 PAM 212 cells using a GenePulser Xcell electroporator (Bio-Rad, Hercules, CA). The host cells were either untreated or irradiated with IR-A 3 hours before electroporation. At 16 hours later, CAT-enzyme activity was measured. Cells were harvested, proteins were purified according to a standard protocol, and the protein concentration was determined using the Bradford method. Total protein (10 µg) was subjected to a CAT-ELISA (Roche Molecular Biochemicals). Mean ± SD absorbance (OD) of one representative experiment out of three independently performed experiments is shown. Statistical analysis was performed using the Student's *t*-test.

Animals

C57BL/6N mice were purchased from Charles River (Sulzfeld, Germany). *Xpa* knockout mice (C57BL/6N background) were generated at the RIVM (de Vries *et al.*, 1995). Animal care was provided by expert personnel in compliance with the relevant laws and institutional guidelines.

Irradiation of mice

Mice were shaved on their backs and exposed to 135 J cm^{-2} IR-A (Hydrosun 505). At 3 hours later, mice were irradiated with UVB (Philips TL12 fluorescent lamps). At 16 hours later, mice were killed. Punch-biopsies (6 mm) were taken from the UV-exposed areas, fixed in 4% formalin, and embedded in paraffin.

Evaluation of sunburn cells

Tissue sections (5 µm) were stained with hematoxylin and eosin. The number of sunburn cells per 6 mm in length of epidermis was counted. The mean ± SD of at least three different sections from one of three independent experiments is shown. The Student's *t*-test was used to test the significance of the differences.

Immunhistochemical staining for CPDs

After deparaffinization of tissue sections (5 µm) with xylol and ethanol at decreasing concentrations, sections were immersed in an aqueous solution containing 0.01 M sodium citrate pH6 and subsequently microwave treated for 10 minutes to unmask antigenic epitopes. Unspecific binding sites were blocked with 10% horse serum and 0.3% saponin in PBS for 10 minutes, followed by incubation at 4 °C overnight with a monoclonal antibody directed against thymine dimers (Kamiya Biomedical Company) at a dilution of 1:500. Endogenous peroxidase activity was blocked by incubation with 3% H_2O_2 for 10 minutes. Staining was performed with an indirect immunoperoxidase technique using the Vectastain Universal quick kit (Vector Labs, Burlingame, CA) and visualized using NovaRed substrate (Vector Labs). Finally, sections were counterstained with hematoxylin. From each sample of two independently

performed experiments, three randomly chosen lengths of 630 µm epidermis were evaluated for the total number of epidermal cells and the number of CPD-positive cells. Results are shown as percentage of CPD-positive cells (mean ± SD). The Student's *t*-test was used to test the significance of the differences.

CONFLICT OF INTEREST
The authors have no commercial associations or other conflicts of interest.

REFERENCES

Applegate LA, Scaletta C, Panizzon R, Frenk E, Hohlfeld P, Schwarzkopf S (2000) Induction of the putative protective protein ferritin by infrared radiation: implications in skin repair. *J Mol Med* 5:247–51

Böhm M, Wolff I, Scholzen TE, Robinson SJ, Healy E, Luger TA *et al.* (2005) alpha-Melanocyte-stimulating hormone protects from ultraviolet radiation-induced apoptosis and DNA damage. *J Biol Chem* 280:5795–802

Cho S, Lee MJ, Kim MS, Lee S, Kim YK, Lee DH *et al.* (2008) Infrared plus visible light and heat from natural sunlight participate in the expression of MMPs and type I procollagen as well as infiltration of inflammatory cell in human skin *in vivo*. *J Dermatol Sci* 50:123–33

Danno K, Horio T, Imamura S (1992) Infrared radiation suppresses ultraviolet B-induced sunburn-cell formation. *Arch Dermatol Res* 284:92–4

Danno K, Mori N, Toda K, Kobayashi T, Utani A (2001) Near-infrared irradiation stimulates cutaneous wound repair: laboratory experiments on possible mechanisms. *Photodermatol Photoimmunol Photomed* 17:261–5

de Laat WL, Jaspers NG, Hoeijmakers JH (1999) Molecular mechanism of nucleotide excision repair. *Genes Dev* 13:768–85

de Vries A, van Oostrom CT, Hofhuis FM, Dortant PM, Berg RJ, de Gruijl FR *et al.* (1995) Increased susceptibility to ultraviolet-B and carcinogens of mice lacking the DNA excision repair gene XPA. *Nature* 377:169–73

Dees C, Harkins J, Petersen MG, Fisher WG, Wachter EA (2002) Treatment of murine cutaneous melanoma with near infrared light. *Photochem Photobiol* 75:296–301

Dover JS, Phillips TJ, Arndt KA (1989) Cutaneous effects and therapeutic uses of heat with emphasis on infrared radiation. *J Am Acad Dermatol* 20:278–86

Frank S, Menezes S, Lebreton-De Coster C, Oster M, Dubretet L, Coulomb B (2006) Infrared radiation induces the p53 signaling pathway: role in infrared prevention of ultraviolet B toxicity. *Exp Dermatol* 15:130–7

Frank S, Oliver L, Lebreton-De Coster C, Moreau C, Lecabellec MT, Michel L *et al.* (2004) Infrared radiation affects the mitochondrial pathway of apoptosis in human fibroblasts. *J Invest Dermatol* 123:823–31

Horwitz LR, Burke TJ, Carnegie D (1999) Augmentation of wound healing using monochromatic infrared energy. Exploration of a new technology for wound management. *Adv Wound Care* 12:35–40

Kim HH, Lee MJ, Kim KH, Cho KH, Eun HC, Chung JH (2005) Augmentation of UV-induced skin wrinkling by infrared irradiation in hairless mice. *Mech Ageing Dev* 126:1170–7

Kim MS, Kim YK, Cho KH, Chung JH (2006) Regulation of type I procollagen and MMP-1 expression after single or repeated exposure to infrared radiation in human skin. *Mech Ageing Dev* 127:875–82

Kligman LH (1982) Intensification of ultraviolet-induced dermal damage by infrared radiation. *Arch Dermatol Res* 272:229–38

Kochevar IE, Pathak MA, Parrish JA (1999) Photophysics, photochemistry, and photobiology. In: *Fitzpatrick's Dermatology in General Medicine*

Freedberg IM, Eisen AZ, Wolff K *et al.* (eds), 5th ed., New York: McGraw-Hill, 220–9

Kulms D, Pöppelmann B, Yarosh D, Luger TA, Krutmann J, Schwarz T (1999) Nuclear and cell membrane effects contribute independently to the induction of apoptosis in human cells exposed to UVB radiation. *Proc Natl Acad Sci USA* 96:7974–9

Kulms D, Zeise E, Pöppelmann B, Schwarz T (2002) DNA damage, death receptor activation and reactive oxygen species contribute to ultraviolet radiation-induced apoptosis in an essential and independent way. *Oncogene* 21:5844–51

Lehman TA, Modali R, Boukamp P, Stanek J, Bennett WP, Welsh JA *et al.* (1993) p53 mutations in human immortalized epithelial cell lines. *Carcinogenesis* 14:833–9

Meffert H, Buchholtz I, Brenke A (1990) Mild infrared A hyperthermia in treatment of systemic scleroderma. *Dermatol Monatsschr* 176:683–6

Möckel F, Hoffmann G, Obermüller R, Drobnik W, Schmitz G (2006) Influence of water-filtered infrared-A (wIRA) on reduction of local fat and body weight by physical exercise. *GMS Ger Med Sci* 4:Doc05

Nickoloff BJ, Qin JZ, Chaturvedi V, Bacon P, Panella J, Denning MF (2002) Life and death signaling pathways contributing to skin cancer. *J Investig Dermatol Symp Proc* 7:27–35

Nishigori C (2006) Cellular aspects of photocarcinogenesis. *Photochem Photobiol Sci* 5:208–14

Owens DW, Knox JM (1978) Influence of heat, wind, and humidity on ultraviolet radiation injury. *Natl Cancer Inst Monogr* 50:161–7

Piazena H, Kelleher D (2008) Comments on ''cellular response to infrared radiation involves retrograde mitochondrial signaling''. *Free Radic Biol Med* 44:1869

Ruven HJ, Berg RJ, Seelen CM, Dekkers JA, Lohman PH, Mullenders LH *et al.* (1993) Ultraviolet-induced cyclobutane pyrimidine dimers are selectively removed from transcriptionally active genes in the epidermis of the hairless mouse. *Cancer Res* 53:1642–5

Schieke S, Stege H, Kürten V, Grether-Beck S, Sies H, Krutmann J (2002) Infrared-A radiation-induced matrix metalloproteinase 1 expression is mediated through extracellular signal-regulated kinase 1/2 activation in human dermal fibroblasts. *J Invest Dermatol* 119:1323–9

Schieke SM, Schroeder P, Krutman J (2003) Cutaneous effects of infrared radiation: from clinical observations to molecular response mechanisms. *Photodermatol Photoimmunol Photomed* 19:228–34

Schramm JM, Warner D, Hardesty RA, Oberg KC (2003) A unique combination of infrared and microwave radiation accelerates wound healing. *Plast Reconstr Surg* 111:258–66

Schroeder P, Krutmann J (2008) *In vivo* relevance of infrared a radiation-induced skin damage: reply to Piazena and Kelleher (Letter to the Editor). *Free Radical Biol Med* 44:1870–1

Schroeder P, Pohl C, Calles C, Marks C, Wild S, Krutmann J (2007) Cellular response to infrared radiation involves retrograde mitochondrial signaling. *Free Radic Biol Med* 43:128–35

Schwarz A, Maeda A, Ständer S, van Steeg H, Schwarz T (2006) IL-18 reduces ultraviolet radiation-induced DNA damage and thereby affects photo-immunosuppression. *J Immunol* 176:2896–901

Schwarz A, Ständer S, Berneburg M, Böhm M, Kulms D, van Steeg H *et al.* (2002) Interleukin-12 suppresses ultraviolet radiation-induced apoptosis by inducing DNA repair. *Nat Cell Biol* 4:26–31

Trautinger F, Kindas-Mügge I, Barlan B, Neuner P, Knobler RM (1995) 72-kD heat shock protein is a mediator of resistance to ultraviolet B light. *J Invest Dermatol* 105:160–2

van der Leun JC, de Gruijl FR (2002) Climate change and skin cancer. *Photochem Photobiol Sci* 1:324–6

Vink AA, Henegouwen B, Nikaido O, Baan RA, Roza L. (1994) Removal of UV-induced DNAlesions in mouse epidermis soon after irradiation. *J Photochem Photobiol B* 24:25–31

Yokoyama K, Oku T (1999) Rheumatoid arthritis-affected temporomandibular joint pain analgesia by linear polarized near infrared irradiation. *Can J Anaesth* 46:683–7